

Screening current effect on the stress and strain distribution in REBCO high-field magnets: experimental verification and numerical analysis

Yufan Yan,¹ Canjie Xin,² Yunfei Tan,³ and Timing Qu¹

¹Department of Mechanical Engineering, Tsinghua University, Beijing 100084, China

²Institute of Modern Physics, Chinese Academy of Sciences, Lanzhou 730000, China

³Wuhan National High Magnetic Field Center, Huazhong University of Science and Technology, Wuhan 430074, China

(Dated: 10 October 2019)

Besides screening-current-induced magnetic fields (SCIF), the shielding effect in high- T_c coated conductors also has a strong influence on its stress/strain distribution in a coil winding, especially during high-field operations. To demonstrate this phenomenon, a special experimental setup was designed. With an LTS background magnet and a small HTS insert coil, we were able to carry out direct observations on the hoop strains of a 10-mm wide REBCO sample. Measured data was compared against numerical solutions solved by electromagnetic models based on T - A formulation and homogeneous mechanical models, showing good agreements. An analytical expression was proposed to estimate the maximum radial Lorentz force considering the shielding effect. Using the developed numerical models, we further studied the potential effects of two of the mostly investigated methods, which were formerly introduced to reduce SCIF, including multi-filamentary conductors and current sweep reversal (CSR) approach.

REBCO ($\text{REBa}_2\text{Cu}_3\text{O}_x$) coated conductors, known as second-generation high temperature superconductors (2G HTS), are promising candidates for future high-field magnets¹. Thanks to advancements in material design and manufacture, higher critical current, better in-field performance, and mechanical strength are being achieved^{2,3}. Considering technical applicability and cost efficiency, the hybrid solution utilizing HTS magnets as insert field boosters is favored by a lot of researchers⁴. Design and experiments on H800, an HTS insert magnet for 1.3 GHz NMR project at MIT, are underway⁵. Upon achieving center field of 27 T in an LTS-HTS system, researchers at Institute of Electrical Engineering (IEE,CAS) launched a new project targeting a 30-T superconducting magnet for quantum oscillation application⁶. At the National High Magnetic Field Laboratory (NHMFL), all superconducting user-magnet with a cold bore size of 34 mm reached the landmark full field of 32 T⁷.

The influence of shielding currents on the magnetic fields of REBCO magnets is widely recognized and studied^{8,9}. It is confirmed by both experimental and numerical studies that the time drift and field distortion brought up by the screening-current-induced magnetic fields (SCIF) deteriorate the overall field quality^{10,11}. Several approaches including filamentation of REBCO tapes and current sweep reversal have been proposed and tested to minimize the negative impacts^{12,13}.

Recently, as is indicated by some studies, when taking the screening effect into account, the non-uniformly distributed currents in REBCO tapes may have a significant impact on the stress and strain distribution^{5,14}, despite its high tolerance for tensile stress¹⁵. In particular, in the pioneer experiment reaching 45.5-T with 14.4-T HTS insert, the one-side wrinkle pattern demonstrated in REBCO tapes also suggests the influence of screening currents¹⁶. But till now, validation experiments conducted in controlled environments are still missing.

To demonstrate this phenomenon, we designed an experiment with simplified structures as illustrated in Fig. 1. A single turn of REBCO tape with a width of 10 mm, provided by Shanghai Superconductor, was prepared to serve as the test

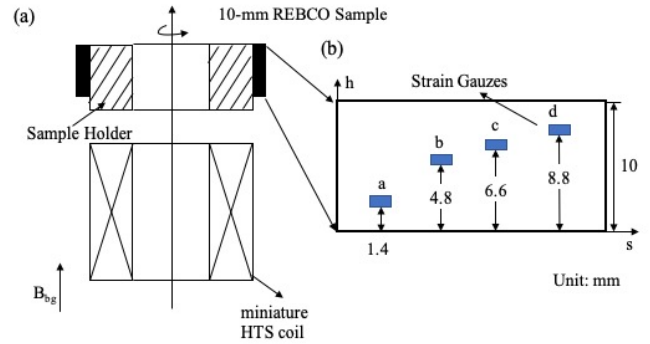


FIG. 1. (a) Experimental setup for in-field strain test. A small HTS coil was co-axially assembled with the sample REBCO tape of 10-mm width, providing dynamic radial field. They were then inserted into an LTS magnet, generating stable parallel field for the sample. (b) Sensors were arranged and numbered a to d from left to right-hand side. Here s and h directions are not plotted in scale.

sample. We attached 4 low-temperature strain gauges (effective width of 1 mm) in total, arranged in an oblique line as shown in Fig. 1(b). Two ends of the sample were welded to the copper terminals on an arc-shaped sample holder with a radius of 17 mm. The sample holder was made of G10, which has a much larger coefficient of thermal contraction comparing to REBCO tape, providing reasonable space for the contraction of the sample while maintaining the structure. A small HTS coil, with inner/outer diameter and winding height of 14 mm, 34 mm and 52 mm, was coaxially aligned to generate the radial fields for the test sample. This whole assembly was then inserted into a low-temperature superconducting magnet with a bore size of 70 mm, providing up to 9.0-T parallel field at the tape surface to magnify the strain response.

With this arrangement, the tested sample was staged in an environment similar to the outermost turn located on the axially outer side of a solenoid coil winding, whereas no transport current was applied. According to the following classic

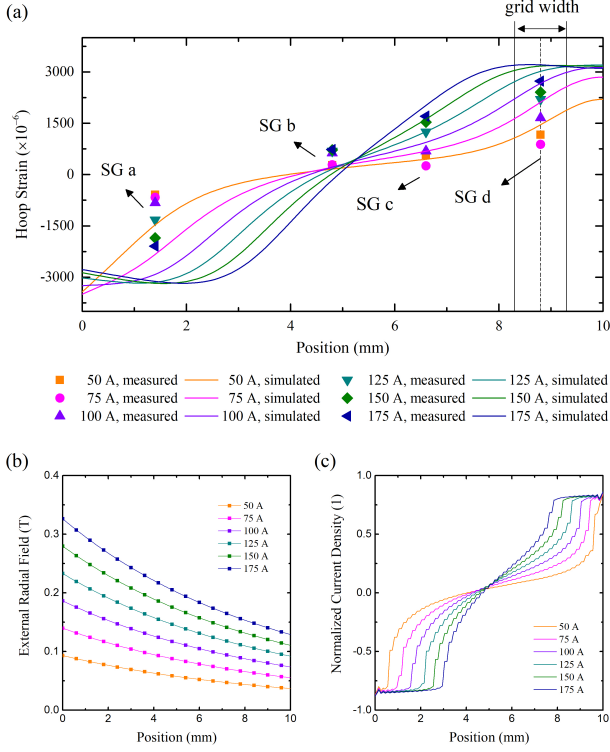


FIG. 2. (a) Measured and calculated hoop strains from strain gauge SG a - SG d, plotted against their axial position in h direction as defined in Fig. 1. Grid width of SG d was marked for reference. (b) Radial external field profile at sample surface. (c) Calculated current distribution.

formula, which is generally used to estimate the hoop stress for high-field magnet design,

$$\sigma = B_z J_\phi r, \quad (1)$$

where B_z is the axial magnetic field for a solenoid coil, J_ϕ is the averaged current density, and r is the radius. Under the assumption of uniform current distribution, hoop stress in this test case should be zero. While, our experiments showed that as the coil was energized, tensile and compressive hoop strains were induced to the sample accordingly (see Fig. 2(a)).

In order to understand its mechanism, numerical models were developed. For electromagnetic fields, we adopted the axisymmetric T - A formulation^{17,18}. The governing equations for the axially aligned superconducting sheet with thin-strip approximation is

$$\frac{d}{dz} E_\phi \left(\frac{dT}{dz} \right) = - \frac{\partial B_r}{\partial t}, \quad (2)$$

where the state variable T is the current vector potential, J is the current density and E is the electrical field. The magnetic field, B then could be incorporated by using A formulation embedded in commercial FEM software. The virtual thickness of the superconducting layer is set to be $1 \mu\text{m}$. The superconducting property is modeled with E - J power law with the

TABLE I. Material properties used in mechanical models.^{19,20}

Material	Thickness	Young's Modulus	Poisson's Ratio
REBCO	$1 \mu\text{m}$	157 GPa	0.3
Copper	$22 \mu\text{m}$	89 GPa	0.34
Hastelloy	$50 \mu\text{m}$	228 GPa	0.307

n -index set as 16, and anisotropic Kim model fitted by experimental data provided by the manufacturer, where J_{c0} , B_0 , k and α are $5.3 \times 10^{11} \text{ A/m}^2$, 0.59 T , 9.1×10^{-3} and 0.60 , respectively.

Then radial Lorentz force profiles are extracted and applied to the axisymmetric elastic model, expressed as

$$f_r = J_\phi B_z, f_z = -J_\phi B_r, \quad (3)$$

where B_r and B_z is the radial and axial magnetic field. Here, the sample is simplified and modeled as four layers with their mechanical properties listed in Tab. I. In consistence with measured hoop strain, thermal contractions are excluded.

The measured and calculated hoop strains when HTS coil was energized with transport currents of 75 A to 175 A were plotted in Fig. 2(a). Reasonable agreements could be obtained. On the axially outer side, tensile hoop strain up to $+2800$ microstrains was observed at sensor d with transport current of 175 A. Contrarily, compressive strains were measured on the opposite side. While near the center, readings at strain gauge b showed minimal changes.

For comparison, radial external field at the sample surface and numerically simulated current distribution are shown in Fig. 2(b) and (c). When subjected to the radial fields generated by the HTS coil, shielding currents were induced in the test sample, in opposite directions near the axially upper and lower side. The frontier of the critical region moved towards the center as the perpendicular fields increased. With the axial field predominately provided by the LTS background magnet, the radial Lorentz force, which contributed the most to the deformation of the sample, presented similar pattern to that of current distribution profile. Hence, along the axially outer rim of the sample, where radially outward Lorentz forces were expected, tensile deformation enlarged with increased external radial fields. While on the opposite side, it showed hoop strains in contraction accordingly.

Without extra reinforcement techniques such as overbanding²¹, Lorentz force in radially outward direction could cause most threat to the outer turns in a solenoid coil winding. Based on previous models and analyses, we propose the following analytical expression to estimate this component of Lorentz force considering screening current effect,

$$f_r \approx J_c(B_r, B_z) B_z, \quad (4)$$

where $J_c(B_r, B_z)$ is the field dependent critical current profile of the tape. The axial field B_z is composed of B_0 , which is contributed by background field magnet, and B^* , which was generated by the insert coil with uniform current distribution

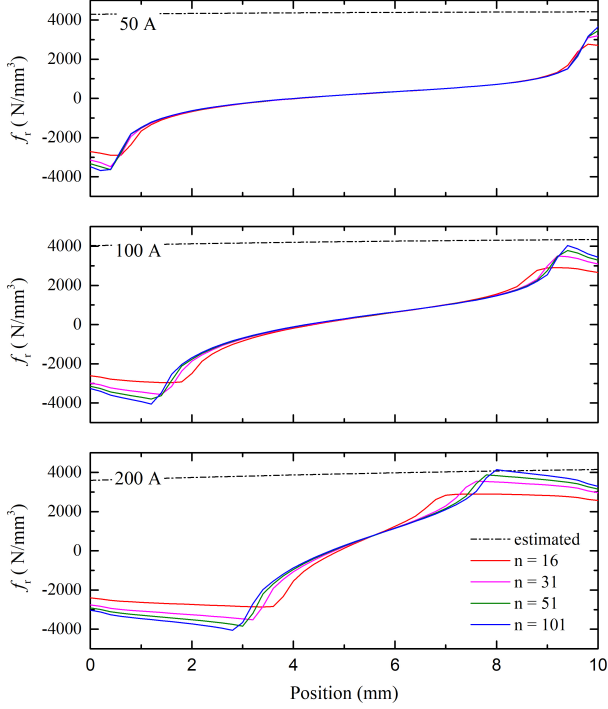


FIG. 3. Radial Lorentz force calculated with n equals to 16, 31, 51 and 101 when the HTS coil was energized with transport current of 50 A, 100 A and 200 A. Estimated values of maximum radial Lorentz force are plotted as well.

assumption and could be obtained by simple static models. In HTS insert magnet design, at the outer turns of a coil winding where the axial fields are dominated by the background magnet, B_z could be further replaced with B_0 .

This could be confirmed by theoretical models. Fig. 3 shows the radial Lorentz force profiles as n is set to be 16, 31, 51 and 101, with the upper bound predicted by the proposed Eq. 4. By taking n -index in E - J power law to an extreme, the solution conforms to that of the critical-state model, with the maximum current density approaching critical current density J_c . These calculations also indicate that, practically, by lowering the value of n , the maximum radial Lorentz force could be reduced, as suggested in Ref. 14.

From Eq. 4, the following conclusion could also be drawn. Although higher critical current density generally implies larger operation margin for current-carrying ability and thermal stability, it could lead to higher radial Lorentz force, limiting its tensile stress margin instead.

Multi-filamentary conductors and current sweep reversal (CSR) are two of the most widely tested approaches to eliminate the SCIF in REBCO magnets^{13,22}. Here we also investigated their effects on the stress and strain distribution using the numerical models we developed. For multi-filamentary REBCO conductors, we modelled samples with 5 and 10 filaments at transport current of 100 A and 200 A for HTS coil, while other parameters were consistent with previous models. As shown in Fig. 4, by constraining shielding effect within fil-

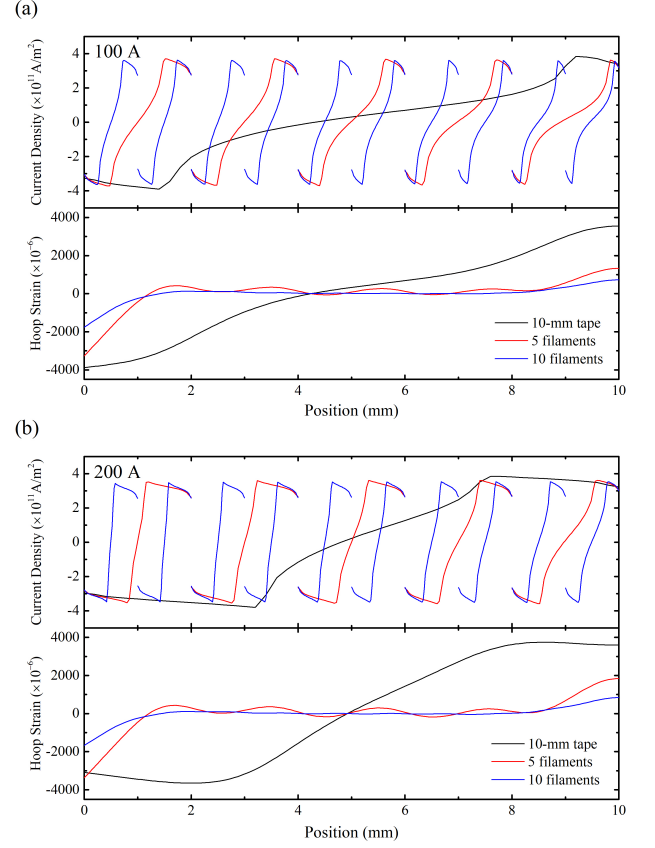


FIG. 4. Calculated current density and hoop strain for samples with 1, 5 and 10 filaments, with transport current of 100 A and 200 A for HTS coil.

aments, electromagnetic forces were distributed equivalently. The tensile hoop strains were effectively mitigated. Specifically, at 200 A, the maximum tensile hoop strain was reduced by factor of 0.51 and 0.77 for 5 and 10 filaments, respectively. But it should also be noted that this type of conductors are generally more prone to mechanical defects introduced during the striation process such as mechanical cutting and laser scribing²³.

For the method of current sweep reversal, we examined the cases of single reverse cycle with the overshooting factors of 10%, 20% and 30%. Target operating current for HTS coil was set at 150 A. Calculated normalized current distribution profiles and hoop strains were summarized in Fig. 5. By overshooting and reverse process, screening currents along sample edges were reversed, and hoop strains at the side previously in tension (right-hand side in Fig. 5) could be lowered down. But with even higher overshooting factor, the opposite rim, which was in compression during normal loading process, could present tensile hoop strain in reverse.

In summary, we experimentally demonstrated the influence of screening current effect on the strain/stress distribution in REBCO coil winding. Numerical modelling with electromagnetic models and mechanical models confirmed this idea. Based on these analyses, we proposed an analytical expression to estimate the maximum radial Lorentz force,

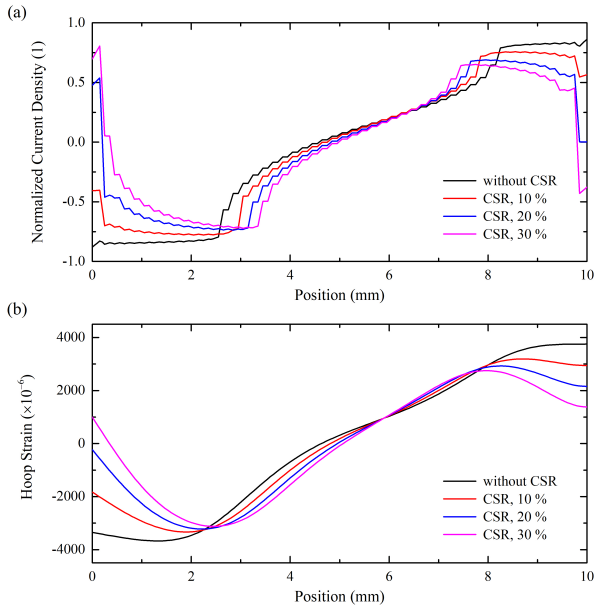


FIG. 5. Calculated hoop strain after single reverse cycle with overshooting factors of 0, 10%, 20% and 30% with target operating current of HTS coils at 150 A.

assisting future REBCO high-field magnet design. Finally, we carried out numerical studies on the effect of filamentized tapes and the method of current sweep reversal, which were previously developed for reducing screening current induced magnetic field. Both showed promising potentials in reducing the influence of screening current effect on the mechanical properties of REBCO magnets.

This work was supported by the Strategic Priority Research Program of Chinese Academy of Sciences under Grant No. XDB25000000 and National Natural Science Foundation of China (U1632276).

- ¹M. Bonura and C. Senatore, "An equation for the quench propagation velocity valid for high field magnet use of REBCO coated conductors," *Applied Physics Letters* **108**, 3–7 (2016).
- ²A. Sundaram, Y. Zhang, A. R. Knoll, D. Abrahimov, P. Brownsey, M. Kasahara, G. M. Carota, R. Nakasaki, J. B. Cameron, G. Schwab, L. V. Hope, R. M. Schmidt, H. Kuraseko, T. Fukushima, and D. W. Hazelton, "2G HTS wires made on 30 μ m thick Hastelloy substrate," *Superconductor Science and Technology* **29**, 104007 (2016).
- ³Y. Zhao, J. Zhu, G. Jiang, C. Cheng, and Y. Yamada, "Progress of second generation high temperature superconducting tape fabrication at shanghai superconductor technology," *Superconductor Science and Technology* (2019).
- ⁴C. Barth, P. Komorowski, R. Tediosi, R. Herzog, R. Schneider, and C. Senatore, "A Size-Constrained 3-T REBCO Insert Coil for a 21-T LTS Magnet: Mechanical Investigations, Conductor Selection, Coil Design, and First Coil Tests," *IEEE Transactions on Applied Superconductivity* **26**, 1–9 (2016).
- ⁵Y. Li, D. Park, Y. Yan, Y. Choi, J. Lee, P. Michael, S. Chen, T.-M. Qu, J. Bascunan, and Y. Iwasa, "Magnetization and screening current in an 800-MHz (18.8-T) REBCO NMR insert magnet: experimental results and

- numerical analysis," *Superconductor Science and Technology* **32** (2019), 10.1088/1361-6668/ab3119.
- ⁶J. Liu, L. Wang, Y. Wang, Q. Wang, and Y. Dai, "Design of a 30-T Superconducting Magnet for Quantum Oscillation Application," *IEEE Transactions on Applied Superconductivity* **29**, 1–5 (2019).
- ⁷H. W. Weijers, W. D. Markiewicz, A. V. Gavrilin, A. J. Voran, Y. L. Viouchkov, S. R. Gundlach, P. D. Noyes, D. V. Abrahimov, H. Bai, S. T. Hanahs, and T. P. Murphy, "Progress in the development and construction of a 32-t superconducting magnet," *IEEE Transactions on Applied Superconductivity* **26**, 1–7 (2016).
- ⁸E. H. Brandt and M. Indenbom, "Type-II-superconductor strip with current in a perpendicular magnetic field," *Physical Review B* **48**, 12893–12906 (1993).
- ⁹Y. Yanagisawa, H. Nakagome, D. Uglietti, T. Kiyoshi, R. Hu, T. Takematsu, T. Takao, M. Takahashi, and H. Maeda, "Effect of YBCO-Coil Shape on the Screening Current-Induced Magnetic Field Intensity," *IEEE Transactions on Applied Superconductivity* **20**, 744–747 (2010).
- ¹⁰S. Noguchi, H. Ueda, S. Hahn, A. Ishiyama, and Y. Iwasa, "A simple screening current-induced magnetic field estimation method for {REBCO} pancake coils," *Superconductor Science and Technology* **32**, 45007 (2019).
- ¹¹E. Pardo, "Modeling of screening currents in coated conductor magnets containing up to 40000 turns," *Superconductor Science and Technology* **29**, 85004 (2016).
- ¹²K. Kajikawa and K. Funaki, "A simple method to eliminate shielding currents for magnetization perpendicular to superconducting tapes wound into coils," *Superconductor Science and Technology* **24**, 125005 (2011).
- ¹³Y. Yanagisawa, Y. Xu, X. Jin, H. Nakagome, and H. Maeda, "Reduction of Screening Current-Induced Magnetic Field of REBCO Coils by the Use of Multi-Filamentary Tapes," *IEEE Transactions on Applied Superconductivity* **25**, 1–5 (2015).
- ¹⁴J. Xia, H. Bai, H. Yong, H. W. Weijers, T. A. Painter, and M. D. Bird, "Stress and strain analysis of a REBCO high field coil based on the distribution of shielding current," *Superconductor Science and Technology* **32** (2019), <https://doi.org/10.1088/1361-6668/ab279c>.
- ¹⁵Y. Iwasa and S. Hahn, "First-cut design of an all-superconducting 100-T direct current magnet," *Applied Physics Letters* **103** (2013), 10.1063/1.4852596.
- ¹⁶S. Hahn, K. Kim, K. Kim, X. Hu, T. Painter, I. Dixon, S. Kim, K. R. Bhattarai, S. Noguchi, J. Jaroszynski, and D. C. Larbalestier, "45.5-tesla direct-current magnetic field generated with a high-temperature superconducting magnet," *Nature* **570**, 496–499 (2019).
- ¹⁷H. Zhang, M. Zhang, and W. Yuan, "An efficient 3D finite element method model based on the T-A formulation for superconducting coated conductors," *Superconductor Science and Technology* **30**, 24005 (2017).
- ¹⁸F. Liang, S. Venuturumilli, H. Zhang, M. Zhang, J. Kvitkovic, S. Pamidi, Y. Wang, and W. Yuan, "A finite element model for simulating second generation high temperature superconducting coils/stacks with large number of turns," *Journal of Applied Physics* **122**, 43903 (2017).
- ¹⁹K. Ilin, K. A. Yagotintsev, C. Zhou, P. Gao, J. Kossé, S. J. Otten, W. A. J. Wessel, T. J. Haugan, D. C. van der Laan, and A. Nijhuis, "Experiments and FE modeling of stress-strain state in REBCO tape under tensile, torsional and transverse load," *Superconductor Science and Technology* **28**, 55006 (2015).
- ²⁰J. W. Ekin and G. O. Zimmerman, *Experimental Techniques for Low-Temperature Measurements: Cryostat Design, Material Properties, and Superconductor Critical-Current Testing* (2006).
- ²¹T. Qu, P. C. Michael, J. Bascuñán, T. Lécrovisse, M. Guan, S. Hahn, and Y. Iwasa, "Test of an 8.66-t rebcO insert coil with overbanding radial build for a 1.3-ghz lts/hts nmr magnet," *IEEE Transactions on Applied Superconductivity* **27**, 1–5 (2017).
- ²²Y. J. Hwang, J. Y. Jang, S. Lee, J. Lee, and W. S. Lee, "Experimental study of the effect of the current sweep cycle on the magnetic field stability of a REBCO coil," *Cryogenics* **89**, 163–167 (2018).
- ²³F. Grilli and A. Kario, "How filaments can reduce AC losses in HTS coated conductors: a review," *Superconductor Science and Technology* **29**, 83002 (2016).